NEOPLASIA
www.neoplasia.com

Volume 11 Number 11 November 2009 pp. 1243–1251 1243

Radiocurability Is Associated with Interstitial Fluid Pressure in Human Tumor Xenografts[1]

Einar K. Rofstad, Jon-Vidar Gaustad, Kjetil G. Brurberg, Berit Mathiesen, Kanthi Galappathi and Trude G. Simonsen

Group of Radiation Biology and Tumor Physiology, Department of Radiation Biology, Institute for Cancer Research, Oslo University Hospital, Oslo, Norway

Abstract

Interstitial fluid pressure (IFP) has been shown to be an independent prognostic parameter for disease-free survival in cervical carcinoma patients treated with radiation therapy. However, the underlying mechanisms are not fully understood. The main aims of this study were to investigate whether tumor radiocurability may be associated with IFP and, if so, to identify possible mechanisms. Human melanoma xenografts transplanted intradermally or in window chamber preparations in BALB/c *nu/nu* mice were used as preclinical tumor models. Radiation dose resulting in 50% local tumor control was higher by a factor of 1.19 ± 0.06 in tumors with IFP ≥ 9 mm Hg than in tumors with IFP ≤ 7 mm Hg. Tumor IFP was positively correlated to vessel segment length and vessel tortuosity and was inversely correlated to vessel density. Compared with tumors with low IFP, tumors with high IFP showed high resistance to blood flow, high frequency of Po_2 fluctuations, and high fractions of acutely hypoxic cells, whereas the fraction of radiobiologically hypoxic cells and the fraction of chronically hypoxic cells did not differ between tumors with high and tumors with low IFP. IFP showed a significant correlation to the fraction of acutely hypoxic cells, probably because both parameters were determined primarily by the microvascular resistance to blood flow. Therefore, the observed association between tumor radiocurability and IFP was most likely an indirect consequence of a strong relationship between IFP and the fraction of acutely hypoxic cells.

Neoplasia (2009) 11, 1243–1251

Introduction

Interstitial fluid pressure (IFP) is generally higher in solid malignant tumors than in the surrounding normal tissue [1]. Most experimental and human tumors show IFP values of 5 to 40 mm Hg, whereas the IFP of most normal tissues ranges from −3 to +3 mm Hg [2]. Elevated IFP in tumors is a consequence of severe microvascular, lymphatic, and interstitial abnormalities [3]. Tumor tissues generally show high geometric and viscous resistance to blood flow, high microvascular hydrostatic pressure, low resistance to transcapillary fluid flow, high resistance to interstitial fluid flow, and impaired lymphatic drainage [3,4]. The microvascular hydrostatic pressure is the principal driving force for interstitial hypertension in tumors [5]. Fluid is forced from the microvasculature into the interstitium where it accumulates, distends the elastic extracellular matrix, and causes an elevation of the IFP [6]. A pseudostable state is established where the central tumor IFP is nearly equal to the microvascular hydrostatic pressure, resulting in reduced fluid flow through the interstitium [7]. One important consequence is poor and heterogeneous uptake of macromolecular therapeutic agents and, hence, tumor resistance to some forms of gene therapy and immunotherapy [8].

Hypoxia is another characteristic feature of the physiological microenvironment of solid malignant tumors [9]. Two main causes of tumor hypoxia have been recognized: permanent limitations in oxygen diffusion result in chronic hypoxia and transient limitations in blood perfusion result in acute hypoxia [10]. Most assays of tumor hypoxia do not distinguish between chronic and acute hypoxia, although the biology of acutely hypoxic cells may differ from that of chronically hypoxic cells [9]. Tumor hypoxia may cause resistance to radiation therapy and some forms of chemotherapy and has been shown to

Abbreviations: GFP, green fluorescence protein; HF, hypoxic fraction; IFP, interstitial fluid pressure; Po_2, oxygen tension; SF, surviving fraction; TCD_{50}, tumor control dose 50, i.e., radiation dose resulting in 50% local tumor control

Address all correspondence to: Einar K. Rofstad, PhD, Group of Radiation Biology and Tumor Physiology, Department of Radiation Biology, Institute for Cancer Research, Norwegian Radium Hospital, Montebello, N-0310 Oslo, Norway.
E-mail: einar.k.rofstad@rr-research.no

[1]This work was supported by the Norwegian Cancer Society.
Received 6 July 2009; Revised 3 August 2009; Accepted 4 August 2009

DOI 10.1593/neo.91152

be associated with malignant progression, increased incidence of metastases, and poor prognosis [10–12]. Clinical studies involving several histologic types of cancer have shown that patients with highly hypoxic primary tumors may have increased frequency of locoregional treatment failure and poor disease-free and overall survival rates after radiation therapy alone or radiation therapy combined with surgery and/or chemotherapy [12–14].

Although the association between outcome of radiation therapy and tumor hypoxia has been investigated in a large number of clinical studies, only one significant clinical study of the association between IFP and patient outcome after radiation therapy has been reported [15,16]. In this study, patients with locally advanced cervical carcinoma were treated with radiation therapy alone, and IFP and oxygen tension (P_{O_2}) were measured in the primary tumor before treatment. The study showed that high IFP was associated with poor disease-free survival independent of conventional prognostic factors, such as tumor size, stage, and lymph node status. Patients with tumors with high IFP had increased probability of developing both local (pelvis) and distant (para-aortic lymph nodes, liver, lungs) recurrences. Interestingly, the independent prognostic impact of IFP for recurrence and survival was strong, whereas the independent prognostic impact of tumor hypoxia was of borderline significance and was limited to patients without nodal metastases [16].

The biological mechanisms by which IFP influences response to radiation treatment, metastasis, and patient survival have not been identified. However, several mechanisms have been suggested, including the possibilities that tumors with high IFP may show a high rate of cell proliferation, large temporal and spatial variations in blood flow and oxygen tension, and a high secretion of cytokines that may stimulate angiogenesis/lymphangiogenesis or cause endothelial cell radiation resistance [3]. Identification of the mechanisms connecting high IFP to poor patient outcome is essential to take full advantage of IFP measurements in cancer diagnostics and treatment. Detailed mechanistic studies can probably be performed only in adequate experimental tumor systems.

Therapeutic and biological consequences of high tumor IFP are currently being investigated in our laboratory by using human melanoma xenografts as preclinical models of human cancer [17,18]. Previously, we have shown that high IFP promotes pulmonary and lymph node metastasis in A-07 tumors by hypoxia-independent mechanisms [18]. The purpose of the work reported here was to investigate whether tumor radiocurability may be associated with IFP. The study was based on the hypothesis that tumors with high IFP may have high fractions of acutely hypoxic cells and, hence, be resistant to radiation treatment. The hypothesis was found to be valid by studying A-07 tumors transplanted intradermally or in window chamber preparations in athymic nude mice. Compared with tumors with low IFP, tumors with high IFP showed high radiation dose resulting in 50% local tumor control (TCD_{50}), high resistance to blood flow, high frequency of P_{O_2} fluctuations, and high fractions of acutely hypoxic cells, whereas the total fraction of hypoxic cells and the fraction of chronically hypoxic cells did not differ between tumors with high and tumors with low IFP.

Materials and Methods

Mice

Adult (8-10 weeks) female BALB/c *nu/nu* mice, bred and maintained as described elsewhere [19], were used as host animals for xenografted tumors. The animal experiments were approved by the institutional committee on research animal care and were done according to the US Public Health Service Policy on Humane Care and Use of Laboratory Animals.

Tumors

A-07 or A-07–green fluorescence protein (GFP) human melanoma xenografts were used as tumor models [20,21]. Intradermal tumors were initiated from monolayer cultures by inoculating aliquots of approximately 3.5×10^5 A-07 cells into the left mouse flank [20]. Window chamber tumors were initiated from A-07-GFP multicellular spheroids with a diameter of 100 to 200 μm [21]. The experiments were carried out when the intradermal tumors had grown to a volume of 250 to 350 mm^3 and when the area of the window chamber tumors was 10 to 15 mm^2.

Anesthesia

Window chamber implantation, intravital microscopy, tumor irradiation, IFP measurements, and P_{O_2} measurements were carried out with anesthetized mice. Fentanyl citrate (Janssen Pharmaceutica, Beerse, Belgium), fluanisone (Janssen Pharmaceutica), and midazolam (Hoffmann-La Roche, Basel, Switzerland) were administered intraperitoneally (IP) in doses of 0.63, 20, and 10 mg/kg, respectively. By using the ^{86}Rb uptake method, it has been verified that this anesthesia does not alter the blood perfusion of A-07 tumors significantly [17]. After window chamber implantation, the mice were given buprenorphine (Temgesic; Schering-Plough, Brussels, Belgium) IP in a dose of 0.12 mg/kg. During experiments, the body core temperature of the mice was kept at 37 to 38°C by using a heating lamp, a heating pad, or a hot air generator.

Window Chamber Preparations and Intravital Microscopy

Window chambers were implanted into the dorsal skin fold of mice as described earlier [21]. Briefly, the chamber consisted of two parallel frames, and after implantation, the frames sandwiched an extended double layer of skin. Before implantation, an approximately 6.0-mm circular hole was made in one of the skin layers. A plastic window with a diameter of 6.0 mm in the frame on the surgical side provided visual access to the tumor growing in the opposite skin layer. Intravital microscopy was carried out by using an inverted fluorescence microscope equipped with filters for green and red lights (IX-71; Olympus, Munich, Germany), a black and white CCD camera (C4742-95; Hamamatsu Photonics, Hamamatsu, Japan), and image acquisition software (Wasabi; Hamamatsu Photonics). Tetramethylrhodamine isothiocyanate–labeled dextran with a molecular weight of 155 kDa (Sigma Aldrich, St. Louis, MO) was used as vascular tracer. After a 0.2-ml bolus of tetramethylrhodamine isothiocyanate–labeled dextran (50 mg/ml) had been injected into the lateral tail vein, the entire vascular network was mapped at a pixel size of 3.4×3.4 μm^2 by transillumination and fluorescence microscopy. Vessel density (vessel length per squared millimeter tumor area), median vessel segment length, and median vessel tortuosity were determined as described elsewhere [21,22].

Interstitial Fluid Pressure Measurements

IFP was measured in the center of tumors by using the wick-in-needle method for intradermal tumors and the Millar SPC 320 catheter for window chamber tumors as described earlier [17,18].

Oxygen Tension Measurements

Tissue Po_2 was measured simultaneously in two positions in each tumor by using a two-channel fiber-optic oxygen-sensing device (OxyLite 2000; Oxford Optronix, Oxford, UK) as described elsewhere [23]. Briefly, after the Po_2 probes had been inserted into the tumor tissue, Po_2 readings were recorded every 5 or 10 seconds for at least 60 minutes and stored. At the end of an experiment, the mouse was killed without withdrawing the probes from the tumor to ensure that the Po_2 dropped rapidly to 0 mm Hg. The mice were watched continuously during Po_2 acquisitions, and if reflex movements occurred during an experiment, the experiment was interrupted and the data discarded. Thirty-eight tumor-bearing mice entered the study, and the Po_2 acquisition was interrupted in two mice because of reflex movements. The following parameters were derived from the Po_2 traces: mean Po_2 (mm Hg), Po_2 fluctuation frequency (number per hour), absolute amplitude of each Po_2 fluctuation (mm Hg), and relative amplitude of each Po_2 fluctuation [23,24]. Previous studies in our laboratory have shown that changes in Po_2 recorded in tumor or muscle tissue during the first 20 minutes after the insertion of an OxyLite probe may represent artifacts caused by the probe [23]. By summing 50 normalized Po_2 traces recorded in A-07 tumors, it was observed that the Po_2 changes recorded within the first 20 minutes were systematic and hence were caused by the probe, whereas those recorded beyond the first 20 minutes were random and hence most likely represented true variations in tissue Po_2 [23]. Therefore, the Po_2 values recorded during the first 20 minutes were excluded from analysis in the present work.

Irradiation

A Stabilipan x-ray unit (Siemens, Erlangen, Germany), operated at 220 kV, 19 to 20 mA, and with 0.5-mm Cu filtration, was used for irradiation. The irradiation was performed by using a dose rate of 5.1 Gy/min and a radiation field of 15 × 15 mm [25]. Hypoxic tumors were obtained by occluding the blood supply with a clamp 5 minutes before the radiation exposure.

TCD_{50} Assay

Tumors were examined twice weekly after irradiation and scored as locally controlled if regrowth was not observed within 90 days after the radiation treatment. The percentage of locally controlled tumors was plotted *versus* radiation dose, and TCD_{50} was determined by probability regression analysis [19]. Probability regression analysis was used because the cumulative distribution function of a normally distributed variable can be shown as a straight line in a probability plot.

Cell Survival Assay

The cell survival of tumors irradiated *in vivo* was measured *in vitro* by using a plastic surface colony assay [19]. Briefly, tumor cell suspensions, prepared by using a standardized mechanical and enzymatic procedure, were plated in tissue culture flasks and incubated for 14 days. The cell surviving fraction of an irradiated tumor was calculated from the plating efficiency of the cells of the tumor and the mean plating efficiency of the cells of six unirradiated tumors. The plating efficiency of the unirradiated control tumors ranged from 30% to 50%.

Fraction of Radiobiologically Hypoxic Cells

The fraction of radiobiologically hypoxic cells was determined for individual tumors by using an experimental procedure based on the paired survival curve method [25]. The tumors were irradiated with 10 Gy under unclamped conditions, and the fraction of surviving cells (SF_{10} [unclamped]) was determined for each tumor as previously mentioned. The fraction of radiobiologically hypoxic cells was calculated as SF_{10} (unclamped)/SF_{10} (clamped), where SF_{10} (clamped) represents the mean cell surviving fraction of ten tumors irradiated with 10 Gy under clamped conditions. The determination of the fraction of radiobiologically hypoxic cells of individual A-07 tumors from measurements of SF_{10} has been justified previously [25]. The theoretical basis for the paired survival curve method has been described in detail by Hall in his textbook on basic radiation biology [26].

Fraction of Chronically Hypoxic Cells

The fraction of chronically hypoxic cells was measured for individual tumors by using a peroxidase-based immunohistochemical assay, optimized with the purpose of staining chronically hypoxic cells adequately without staining normoxic or acutely hypoxic cells significantly. The assay and a critical evaluation of the assay have been reported elsewhere [25]. Briefly, pimonidazole [1-[(2-hydroxy-3-piperidinyl)-propyl]-2-nitroimidazole], a well-characterized hypoxia marker [27], was administered IP in doses of 30 mg/kg 4 hours before tumor resection. Histologic preparations, produced from tumor tissue fixed in phosphate-buffered 4% paraformaldehyde, were incubated with polyclonal rabbit antiserum to pimonidazole-protein adducts. Diaminobenzidine was used as a chromogen, and hematoxylin was used for counterstaining. Quantitative studies of hypoxia were based on six cross sections of each tumor. The fraction of chronically hypoxic cells (i.e., the area fraction of the tissue showing positive pimonidazole staining) was determined by image analysis.

Fraction of Acutely Hypoxic Cells

The fraction of acutely hypoxic cells (HF_{Acu}) was calculated from the fraction of radiobiologically hypoxic cells (HF_{Rad}) and the fraction of chronically hypoxic cells (HF_{Chr}) as $HF_{Acu} = HF_{Rad} - HF_{Chr}$. Thus, HF_{Rad}, HF_{Chr}, and the difference between HF_{Rad} and HF_{Chr} were assumed to represent the total fraction of hypoxic cells, the fraction of chronically hypoxic cells, and the fraction of acutely hypoxic cells, respectively. These assumptions have been verified to be valid for human melanoma xenografts [25,28,29].

Statistical Analysis

Correlations between variables were searched for by regression analysis (linear correlations) or by using the Spearman rank-order correlation test (nonlinear correlations). Statistical comparisons of data were carried out by using the Student's *t* test when the data complied with the conditions of normality and equal variance and otherwise by nonparametric analysis using the Mann-Whitney rank sum test. Probability values of $P < .05$, determined from two-sided tests, were considered significant. The statistical analysis was performed by using the SigmaStat statistical software (Jandel Scientific GmbH, Erkrath, Germany).

Results

The Radiocurability of A-07 Tumors Is Associated with IFP

To investigate whether tumor radiocurability may be associated with IFP, TCD_{50} was determined for intradermal A-07 tumors with low IFP (IFP ≤ 7 mm Hg) and high IFP (IFP ≥ 9 mm Hg). Two hundred tumor-bearing mice were included in the experiment. The volume of

the tumors with low IFP (312 ± 19 mm^3) was not significantly different from that of the tumors with high IFP (303 ± 22 mm^3; $P > .05$). IFP was measured immediately before the tumors were exposed to single-dose irradiation. TCD_{50} was found to be higher for tumors with high IFP than for tumors with low IFP by a factor of 1.19 ± 0.06 (Figure 1; $P = .000049$). The numerical values of TCD_{50} (mean [95% confidence interval]) for the two tumor groups were 37.7 Gy (34.8-40.4 Gy) and 31.7 Gy (29.5-33.4 Gy).

IFP Is Correlated to Vessel Segment Length and Vessel Tortuosity and Inversely Correlated to Vessel Density in A-07-GFP Tumors

To explore possible mechanisms leading to high IFP in tumors, the morphology of the microvascular network was characterized for five A-07-GFP window chamber tumors varying widely in IFP. Qualitative studies revealed that the network differed substantially between tumors with low IFP and tumors with high IFP (Figure 2*A*). Quantitative analysis showed that IFP decreased with increasing vessel density and increased with increasing vessel segment length and increasing vessel tortuosity (Figure 2*B*). Significant correlations were found between IFP and vessel density ($P = .0084$) and IFP and vessel segment length ($P = .017$), whereas the relationship between IFP and vessel tortuosity was of borderline significance ($P = .083$).

High IFP Is Associated with a High Frequency of Po_2 Fluctuations in A-07 Tumors

To search for possible associations between IFP and Po_2, IFP and Po_2 were recorded in the same intradermal A-07 tumors. Thirty-six tumors were included in the experiment. Median IFP of the tumors was 7.3 mm Hg. The volume of the tumors with IFP below the median value (306 ± 23 mm^3) was not significantly different from that of the tumors with IFP above the median value (293 ± 27 mm^3; $P > .05$). The Po_2 traces differed substantially between tumors with low IFP and tumors with high IFP (Figure 2*C*). The tumors with IFP above the median value showed a higher frequency of Po_2 fluctuations than the tumors with IFP below the median value (Figure 2*D*; $P = .031$). Mean Po_2 and the absolute and relative amplitudes of the Po_2 fluctuations did not differ between the two tumor groups ($P > .05$ for all parameters). The Po_2 traces showed no general trend for increasing or decreasing Po_2 with time. The numerical values derived from the first 20 minutes of the Po_2 traces were not significantly different from those derived from the last 20 minutes, regardless of whether mean Po_2, Po_2 fluctuation frequency, absolute amplitude of each Po_2 fluctuation, or relative amplitude of each Po_2 fluctuation was considered ($P > .05$ for all parameters).

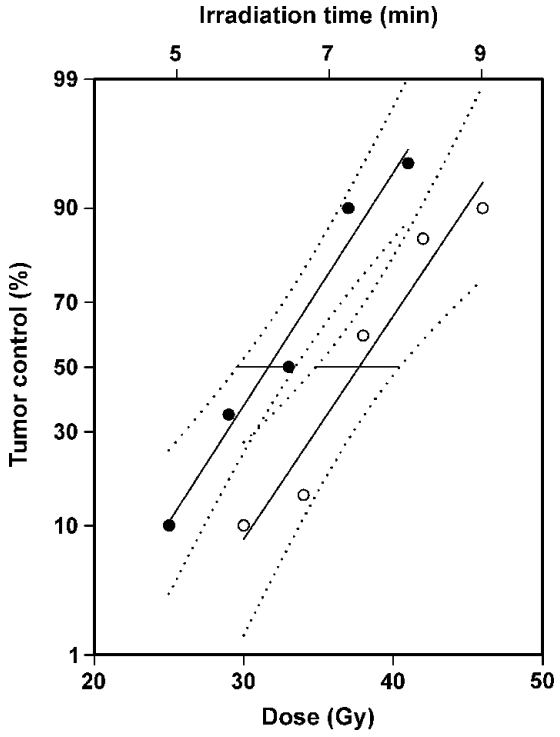

Figure 1. Local tumor control *versus* radiation dose and irradiation time for intradermal A-07 tumors with IFP ≤ 7 mm Hg (●) and IFP ≥ 9 mm Hg (○). Points indicate percentage of locally controlled tumors, based on 20 tumor-bearing mice; solid curves, curves fitted to the data by probability regression analysis; dotted curves, 95% confidence intervals; horizontal lines, the 95% confidence intervals of TCD_{50}.

IFP Is Correlated to the Fraction of Acutely Hypoxic Cells But Not to the Fraction of Radiobiologically Hypoxic Cells or to the Fraction of Chronically Hypoxic Cells in A-07 Tumors

To investigate whether IFP may be correlated to the fraction of radiobiologically hypoxic cells, the fraction of chronically hypoxic cells, and/or the fraction of acutely hypoxic cells, these four parameters were determined for 20 intradermal A-07 tumors. IFP was recorded immediately before the tumors were exposed to a single radiation dose of 10 Gy under unclamped conditions. After the radiation exposure, the tumors were resected and cut into approximately 1-mm-thick slices. One half of each tumor (every second slice) was processed for measurement of SF_{10} (unclamped) and the fraction of radiobiologically hypoxic cells, whereas the other half was processed for detection of pimonidazole-positive cells and assessment of the fraction of chronically hypoxic cells. The fraction of acutely hypoxic cells was then calculated as described above.

SF_{10} (unclamped) differed by a factor of approximately 75, from 4.5×10^{-4} to 3.4×10^{-2}, among the 20 tumors, whereas SF_{10} (clamped) of 10 control tumors and SF_{20} (clamped) of 10 control tumors differed by factors of approximately 1.8 and 2.2, respectively (Figure 3). The geometric means of SF_{10} (unclamped), SF_{10} (clamped), and SF_{20} (clamped), indicated by horizontal lines in Figure 3, were 1.1×10^{-2}, 9.0×10^{-2}, and 1.4×10^{-3}, respectively. The coefficients of variation were 69% (SF_{10} [unclamped]), 17% (SF_{10} [clamped]), and 25% (SF_{20} [clamped]). The differences in SF_{10} (unclamped) among the tumors thus primarily reflected differences in the fraction of radiobiologically hypoxic cells and not experimental uncertainty. The fraction of radiobiologically hypoxic cells differed from 0.5% to 37.6%, with a geometric mean of 12% and an arithmetic mean of 17%.

The fraction of chronically hypoxic cells differed among the 20 tumors from 0.0% to 31.5% with mean and median values of 8.2% and 4.8%, respectively. The fraction of acutely hypoxic cells was higher than the fraction of chronically hypoxic cells in 13 of the 20 tumors and ranged from 0.5% to 35.1% with mean and median values of 8.8% and 5.3%, respectively. There was no positive or inverse correlation between the fraction of acutely hypoxic cells and the fraction of chronically hypoxic cells in the tumors (Figure 4; $P > .05$).

IFP differed among the 20 tumors from 2.0 to 17.5 mm Hg with a median value of 8.0 mm Hg. The tumors with IFP above the median value did not differ from those with IFP below the median value

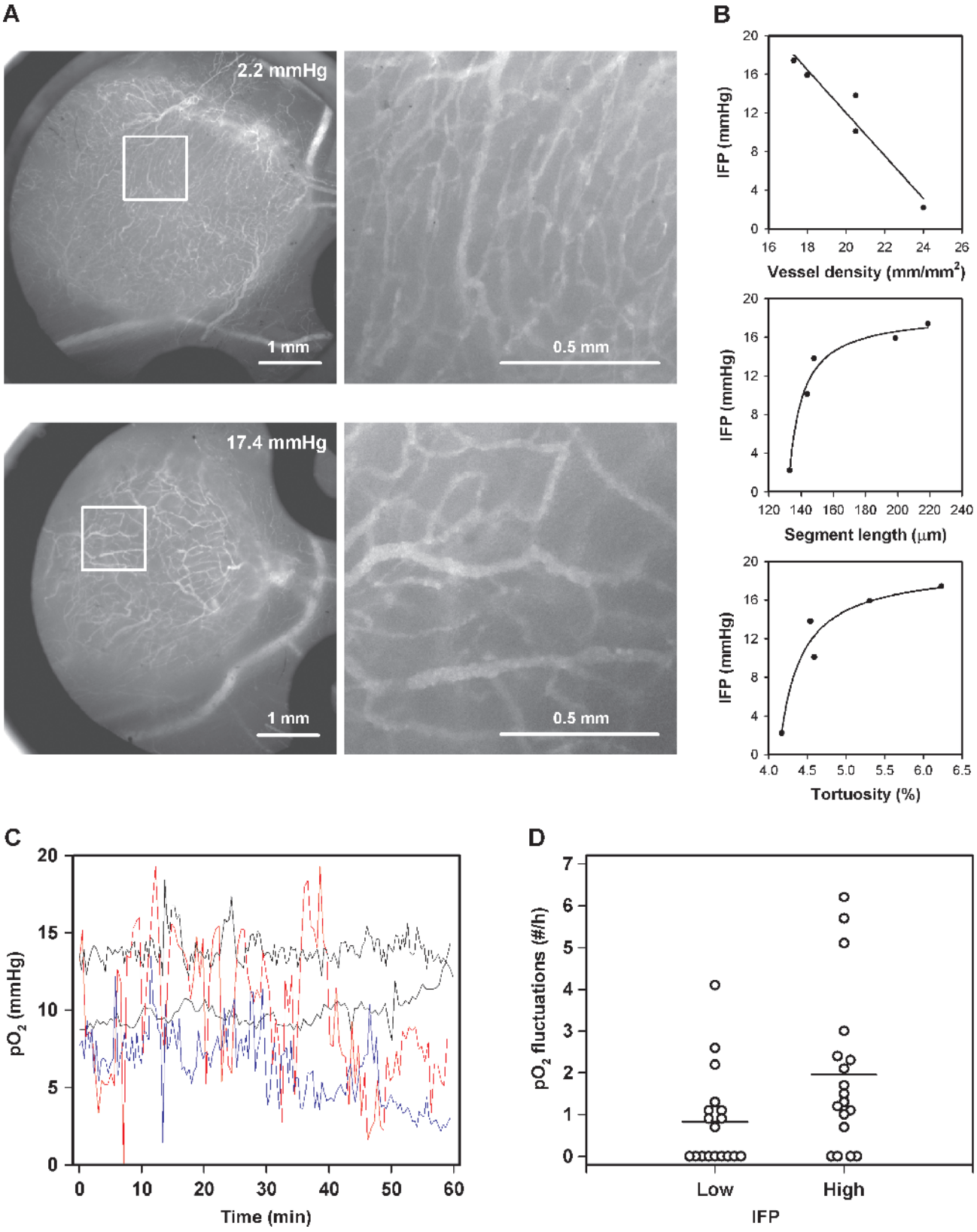

Figure 2. (A) Vascular morphology of two A-07-GFP window chamber tumors with IFP of 2.2 and 17.4 mm Hg shown at low (left) and high (right) magnifications. (B) IFP *versus* vessel density, median vessel segment length, and median vessel tortuosity for A-07-GFP window chamber tumors. Points indicate individual tumors; curves, curves fitted to the data by regression analysis. (C) Representative Po_2 traces for intradermal A-07 tumors with low (black curves) or high (red and blue curves) IFP. Time zero refers to 20 minutes after the probe insertion because the Po_2 values recorded before this time point were influenced by artifacts caused by the probe and hence were excluded from analysis. (D) Po_2 fluctuation frequency for intradermal A-07 tumors with IFP $<$ 7.3 mm Hg (low) and IFP $>$ 7.3 mm Hg (high). Points indicate individual tumors; horizontal lines, mean values.

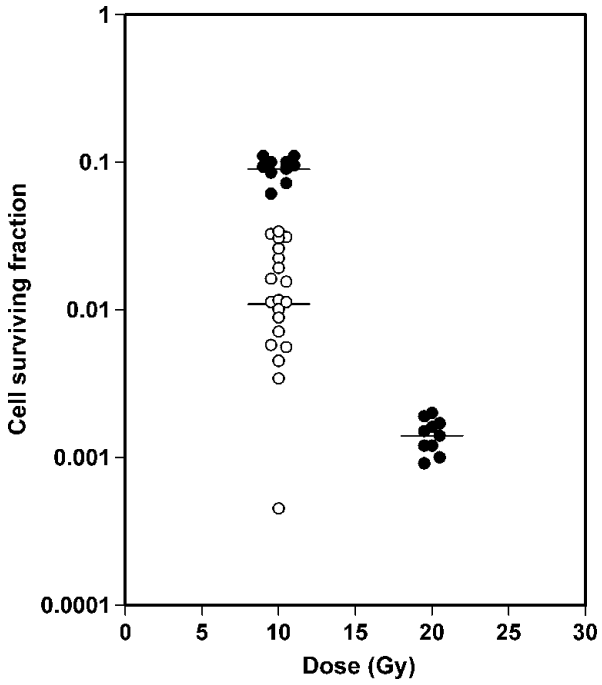

Figure 3. Cell surviving fraction *versus* radiation dose for intradermal A-07 tumors irradiated under clamped (●) or unclamped conditions (○). Points indicate individual tumors; horizontal lines, geometric means.

in the fraction of radiobiologically hypoxic cells (Figure 5*A*; $P > .05$) or in the fraction of chronically hypoxic cells (Figure 5*A*; $P > .05$), whereas the fraction of acutely hypoxic cells was higher for the tumors with high IFP than for those with low IFP (Figure 5*A*; $P = .038$). Furthermore, there was no correlation between IFP and the fraction of radiobiologically hypoxic cells (Figure 5*B*; $P > .05$) or between IFP and the fraction of chronically hypoxic cells (Figure 5*B*; $P > .05$). Conversely, IFP increased linearly with the increasing fraction of acutely hypoxic cells (Figure 5*B*; $P = .000014$).

Discussion

The radiocurability of tumors has been shown to depend on several biological and physiological parameters, including number of clonogenic cells, fraction of hypoxic cells, rate of cell proliferation, and cellular radiation sensitivity [30]. The present work shows that tumor radiocurability also may be associated with IFP. In A-07 human melanoma xenografts, TCD_{50} was found to be significantly higher for tumors with high IFP than for tumors with low IFP. This is a novel observation that may have significant implications for the radiation therapy of cancer. Furthermore, the main underlying mechanism was identified by studying relationships between IFP and P_{O_2} fluctuations using fiber-optic oxygen-sensing probes, between IFP and hypoxia using assays discriminating between chronically and acutely hypoxic cells, and between IFP and microvascular morphology using tumors transplanted into dorsal skin fold window chambers.

The A-07 melanoma line was chosen for this study for several reasons. It has been shown that the experimental procedures used here give highly reproducible results for tumors of this line, and the underlying assumptions have been verified to be valid for A-07 tumors [17–25,28,29]. Moreover, the IFP of A-07 tumors can be measured reliably in a single location in the tumor center because the IFP is uniform throughout the tumors except close to the surface, where it drops precipitously to normal tissue values [18]. Finally, A-07 tumors of the size used here do not develop regions with necrotic tissue and show fractions of chronically hypoxic cells and fractions of acutely hypoxic cells that are of approximately the same magnitude [25,28,29].

On the basis of previous experience with A-07 tumors [31], the TCD_{50} values reported here were obtained by using a dose rate of 5.1 Gy/min and single-radiation doses ranging from 25 to 46 Gy, implying that the exposure time varied among the tumors from approximately 5 to 9 minutes. In comparison, the number of P_{O_2} fluctuations per hour varied between 0 and 7, and consistent with previous studies [23], the duration of the acute hypoxia periods was short compared with the irradiation times. Thus, most periods in which P_{O_2} was acutely less than 5 mm Hg had a duration of less than 2 minutes. Furthermore, the P_{O_2} fluctuations recorded simultaneously in two different positions in the tumors were not coordinated as described previously for A-07 tumors [23]. Consequently, it is unlikely that the fractional time the tumor cells were acutely hypoxic during the radiation exposure varied consistently with the radiation dose and thus influenced the TCD_{50} values. It should also be noticed that similar dose ranges were used for tumors with low IFP and tumors with high IFP.

A-07 window chamber tumors with high IFP showed low vessel density, long vessel segment lengths, and high vessel tortuosity. Tortuous and elongated vessels resist blood flow, are often leaky, and may cause hemoconcentration and intravascular coagulation [32]. Tumor microvascular networks characterized by long vessel segment lengths and high vessel tortuosity have high viscous and geometric resistance to blood flow, high intravessel hydrostatic pressure, and show low blood flow velocities [32,33]. Consequently, high IFP in A-07 tumors was most likely a result of high microvascular hydrostatic pressure and low resistance to transcapillary fluid flow caused by severe morphologic abnormalities in the microvascular network. This suggestion is consistent with earlier studies having shown that the microvasculature of A-07 tumors has a high frequency of endothelial

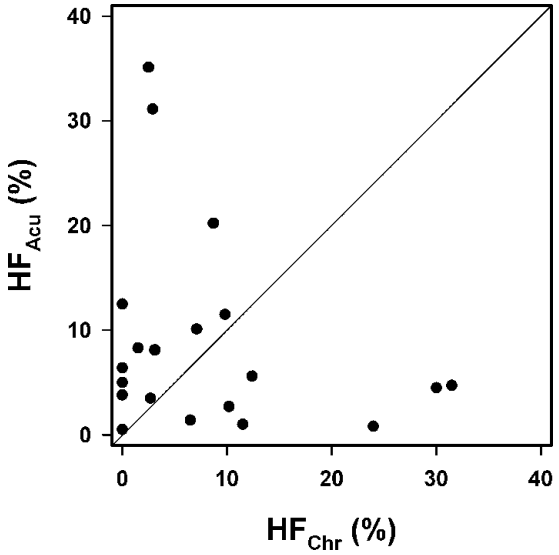

Figure 4. Fraction of acutely hypoxic cells (HF_{Acu}) *versus* the fraction of chronically hypoxic cells (HF_{Chr}) for intradermal A-07 tumors. Points indicate individual tumors; line, line indicating $HF_{Acu} = HF_{Chr}$.

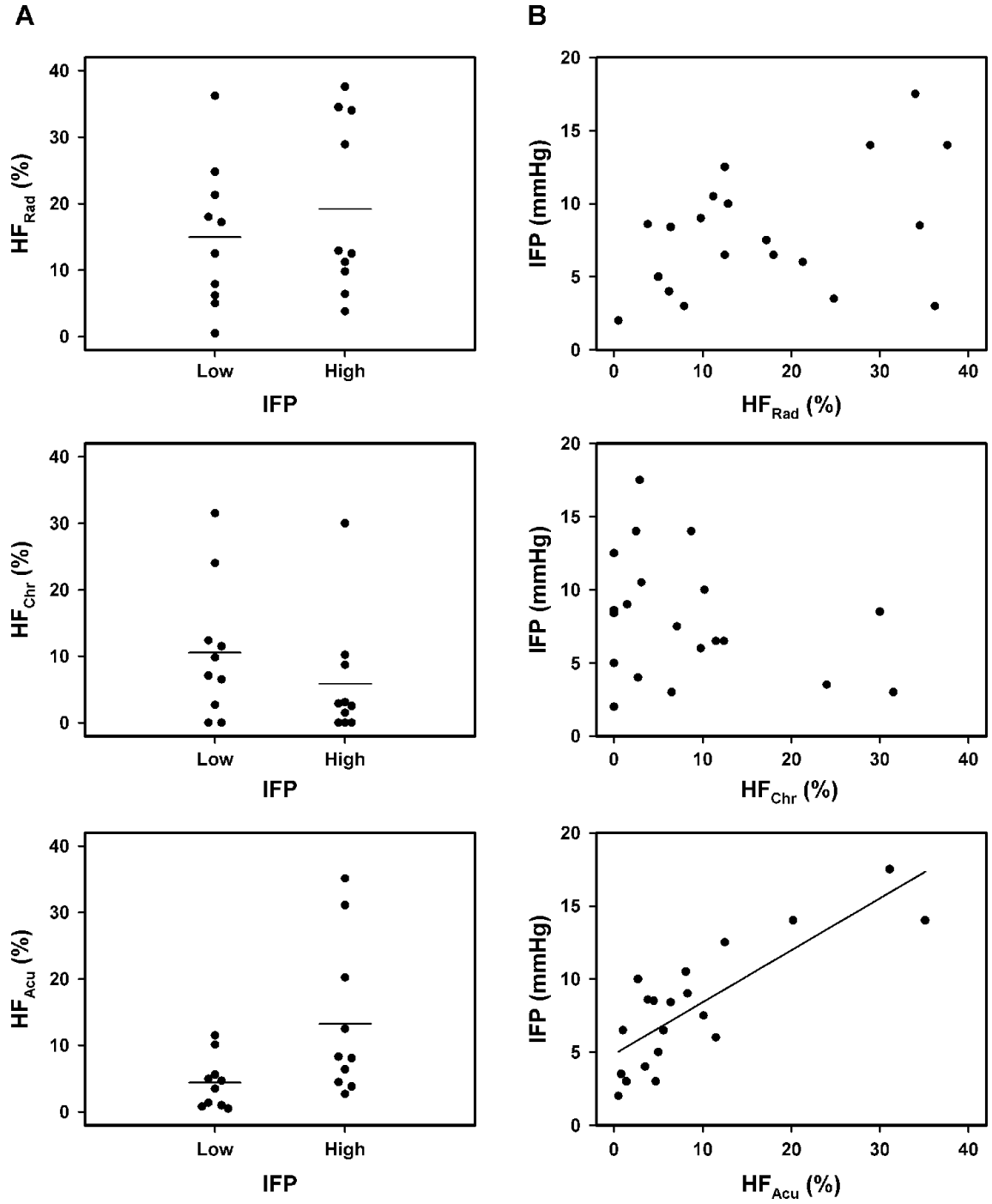

Figure 5. (A) The fraction of radiobiologically hypoxic cells (HF_{Rad}), the fraction of chronically hypoxic cells (HF_{Chr}), and the fraction of acutely hypoxic cells (HF_{Acu}) for intradermal A-07 tumors with IFP < 8.0 mm Hg (low) and IFP > 8.0 mm Hg (high). Points indicate individual tumors; horizontal lines, mean values. (B) IFP *versus* HF_{Rad}, HF_{Chr}, and HF_{Acu} for intradermal A-07 tumors. Points indicate individual tumors; curve, curve fitted to the data by linear regression analysis.

fenestrae and large interendothelial gaps, incomplete endothelial lining, and discontinuous basement membrane [20] and shows high effective permeability constants for macromolecules [34,35].

Furthermore, A-07 tumors with high IFP showed a high frequency of P_{O_2} fluctuations. Fluctuations in P_{O_2} in tumors are primarily a result of fluctuations in blood flow [36]. Previous studies have shown that fluctuations in microvessel blood flow occur frequently in A-07 tumors and are due to vasomotor activity in tumor-supplying arterioles, mechanical compression of vessel walls caused by proliferating tumor cells, intravascular stasis and clot formation, and vessel obstruction caused by circulating white blood cells [37]. It is conceivable that tumors with high resistance to blood flow show a particularly high frequency of blood flow fluctuations [36]. Consequently, the association between high IFP and high frequency of P_{O_2} fluctuations was most likely a result of both parameters being determined primarily by the geometric and viscous resistance to blood flow.

The association between tumor radiocurability and IFP observed here may thus be explained in the following way. First, high geometric

and viscous resistance to blood flow resulted in a high microvascular hydrostatic pressure, and high microvascular hydrostatic pressure and low transvascular resistance to fluid flow resulted in high IFP. Second, high geometric and viscous resistance to blood flow resulted in low blood flow velocity and high frequency of blood flow fluctuations, high frequency of blood flow fluctuations resulted in a high frequency of P_{O_2} fluctuations, a high frequency of P_{O_2} fluctuations resulted in high fractions of acutely hypoxic cells, and high fractions of acutely hypoxic cells resulted in high TCD_{50}. Therefore, the present association between high IFP and high TCD_{50} was most likely primarily an indirect consequence of a strong correlation between the fraction of acutely hypoxic cells and IFP.

Earlier studies have also investigated the relation between the IFP of tumors and tumor oxygenation, both in patients with cervical carcinoma [15,16] and in experimental tumor models [38–40]. These studies failed to demonstrate any correlation between IFP and hypoxia, possibly because tumor hypoxia was assessed with assays that do not discriminate between chronic and acute hypoxia. The observations reported here are thus not inconsistent with these earlier studies. Also, in the present study, there was no correlation between IFP and total fraction of hypoxic cells as assessed by a radiobiological assay.

The geometric resistance to blood flow in the microvasculature of tumors is a complex function of the geometric resistance of the individual vessel segments and the overall architecture of the network [32]. Several morphologic and architectural parameters influencing the geometric resistance have been identified and quantitated [1,6]. However, to our knowledge, quantitative studies linking geometric resistance to blood flow, and hence IFP, to multiple microvascular parameters have not been reported for any tumor thus far. The IFP of the A-07 window chamber tumors studied here ranged from 2.2 to 17.4 mm Hg. This nearly eight-fold difference in IFP was coupled to an approximately 0.7-fold difference in vessel density, a 1.6- to 1.7-fold difference in vessel segment length, and an approximately 1.5-fold difference in vessel tortuosity. This observation suggests that relatively modest differences among tumors in microvascular parameters may lead to significant differences in geometric resistance to blood flow and, hence, significant differences in IFP.

Clinical studies have suggested that tumor IFP may be a strong prognostic parameter for patients treated with radiation therapy [15,16]. Associations between patient outcome and IFP may be an indirect result of associations between patient outcome and tumor oxygenation because the present work suggests that high IFP and high fraction of acutely hypoxic cells in tumors may have high resistance to blood flow as a common cause, and associations between tumor radiocurability and IFP may be an indirect consequence of associations between tumor radiocurability and fraction of acutely hypoxic cells. However, high IFP may also have impacts on patient outcome, which are independent of tumor hypoxia. Studies in our laboratory have thus shown that high IFP in the primary tumor promotes pulmonary and lymph node metastasis in small human melanoma xenografts without hypoxic cells [18]. It is also highly unlikely that the poor and heterogeneous uptake of macromolecular chemotherapeutic agents seen in tumors with high IFP is influenced significantly by acute hypoxia *per se* [8]. Furthermore, the present work does, of course, not exclude the possibility that high IFP also may influence tumor radiocurability by hypoxia-independent mechanisms.

Our observation that both high IFP and high fraction of acutely hypoxic cells in tumors may be a consequence of long vessel segment lengths and high vessel tortuosity, gives strong support to the suggestion that the tumor microvascular network may be an important target for novel therapeutic strategies. The antivascular therapeutic strategies currently under development aim at inhibiting angiogenesis, disrupting the microvascular network, or normalizing the microvasculature [41]. Viewed in the light of the observations reported here, strategies making use of antiangiogenic agents that may normalize the microvasculature are particularly interesting, also because it has been shown that the treatment of cancer with such agents may decrease tumor IFP and improve tumor oxygenation [42].

In summary, high TCD_{50} was found to be associated with high IFP in A-07 human melanoma xenografts. This association was probably an indirect consequence of a significant correlation between IFP and the fraction of acutely hypoxic cells. The correlation between IFP and the fraction of acutely hypoxic cells was most likely a result of both parameters being determined primarily by the vessel segment length and the vessel tortuosity and, hence, the geometric and viscous resistance to blood flow. These observations suggest that associations between treatment outcome and tumor IFP for patients given radiation therapy may be an indirect result of associations between patient outcome and tumor oxygenation.

Acknowledgments

The authors thank Kristin Henriksen, Edrun Andrea Schnell, Kristil Kindem, and Else-Beate M. Ruud for technical assistance.

References

[1] Heldin CH, Rubin K, Pietras K, and Östman A (2004). High interstitial fluid pressure—an obstacle in cancer therapy. *Nat Rev Cancer* **4**, 806–813.
[2] Fukumura D and Jain RK (2007). Tumor microenvironment abnormalities: causes, consequences, and strategies to normalize. *J Cell Biochem* **101**, 937–949.
[3] Lunt SJ, Fyles A, Hill RP, and Milosevic M (2008). Interstitial fluid pressure in tumors: therapeutic barrier and biomarker of angiogenesis. *Future Oncol* **4**, 793–802.
[4] Cairns R, Papandreou I, and Denko N (2006). Overcoming physiologic barriers to cancer treatment by molecularly targeting the tumor microenvironment. *Mol Cancer Res* **4**, 61–70.
[5] Boucher Y and Jain RK (1992). Microvascular pressure is the principal driving force for interstitial hypertension in solid tumors: implications for vascular collapse. *Cancer Res* **52**, 5110–5114.
[6] Milosevic M, Fyles A, and Hill RP (1999). The relationship between elevated interstitial fluid pressure and blood flow in tumors: a bioengineering analysis. *Int J Radiat Oncol Biol Phys* **43**, 1111–1123.
[7] Milosevic M, Fyles A, Hedley D, and Hill RP (2004). The human tumor microenvironment: invasive (needle) measurement of oxygen and interstitial fluid pressure. *Semin Radiat Oncol* **14**, 249–258.
[8] Jain RK (1996). Delivery of molecular medicine to solid tumors. *Science* **271**, 1079–1080.
[9] Höckel M and Vaupel P (2001). Tumor hypoxia: definitions and current clinical, biologic, and molecular aspects. *J Natl Cancer Inst* **93**, 266–276.
[10] Brown JM and Giaccia AJ (1998). The unique physiology of solid tumors: opportunities (and problems) for cancer therapy. *Cancer Res* **58**, 1408–1416.
[11] Rofstad EK (2000). Microenvironment-induced cancer metastasis. *Int J Radiat Biol* **76**, 589–605.
[12] Harris AL (2002). Hypoxia—a key regulatory factor in tumour growth. *Nat Rev Cancer* **2**, 38–47.
[13] Vaupel P (2004). Tumor microenvironmental physiology and its implications for radiation oncology. *Semin Radiat Oncol* **14**, 198–206.
[14] Vaupel P and Mayer A (2007). Hypoxia in cancer: significance and impact on clinical outcome. *Cancer Metastasis Rev* **26**, 225–239.
[15] Milosevic M, Fyles A, Hedley D, Pintilie M, Levin W, Manchul L, and Hill RP (2001). Interstitial fluid pressure predicts survival in patients with cervix cancer independent of clinical prognostic factors and tumor oxygen measurements. *Cancer Res* **61**, 6400–6405.
[16] Fyles A, Milosevic M, Pintilie M, Syed A, Levin W, Manchul L, and Hill RP (2006). Long-term performance of interstitial fluid pressure and hypoxia as prognostic factors in cervix cancer. *Radiother Oncol* **80**, 132–137.

[17] Gulliksrud K, Brurberg KG, and Rofstad EK (2009). Dynamic contrast-enhanced magnetic resonance imaging of tumor interstitial fluid pressure. *Radiother Oncol* **91**, 107–113.

[18] Rofstad EK, Tunheim SH, Mathiesen B, Graff BA, Halsør EF, Nilsen K, and Galappathi K (2002). Pulmonary and lymph node metastasis is associated with primary tumor interstitial fluid pressure in human melanoma xenografts. *Cancer Res* **62**, 661–664.

[19] Rofstad EK (1991). Influence of cellular radiation sensitivity on local tumor control of human melanoma xenografts given fractionated radiation treatment. *Cancer Res* **51**, 4609–4612.

[20] Rofstad EK (1994). Orthotopic human melanoma xenograft model systems for studies of tumour angiogenesis, pathophysiology, treatment sensitivity and metastatic pattern. *Br J Cancer* **70**, 804–812.

[21] Gaustad JV, Simonsen TG, Brurberg KG, Huuse EM, and Rofstad EK (2009). Blood supply in melanoma xenografts is governed by the morphology of the supplying arteries. *Neoplasia* **11**, 277–285.

[22] Gaustad JV, Brurberg KG, Simonsen TG, Mollatt CS, and Rofstad EK (2008). Tumor vascularity assessed by magnetic resonance imaging and intravital microscopy imaging. *Neoplasia* **10**, 354–362.

[23] Brurberg KG, Graff BA, and Rofstad EK (2003). Temporal heterogeneity in oxygen tension in human melanoma xenografts. *Br J Cancer* **89**, 350–356.

[24] Brurberg KG, Graff BA, Olsen DR, and Rofstad EK (2004). Tumor-line specific P_{O_2} fluctuations in human melanoma xenografts. *Int J Radiat Oncol Biol Phys* **58**, 403–409.

[25] Rofstad EK and Måseide K (1999). Radiobiological and immunohistochemical assessment of hypoxia in human melanoma xenografts: acute and chronic hypoxia in individual tumours. *Int J Radiat Biol* **75**, 1377–1393.

[26] Hall E (2000). *Radiobiology for the Radiologist.* Philadelphia, PA: Lippincott Williams & Wilkins.

[27] Raleigh JA, Dewhirst MW, and Thrall DE (1996). Measuring tumor hypoxia. *Semin Radiat Oncol* **6**, 37–45.

[28] Gulliksrud K, Vestvik IK, Galappathi K, Mathiesen B, and Rofstad EK (2008). Detection of hypoxic cell subpopulations in human melanoma xenografts by pimonidazole immunohistochemistry. *Radiat Res* **170**, 638–650.

[29] Rofstad EK, Galappathi K, Mathiesen B, and Ruud EBM (2007). Fluctuating and diffusion-limited hypoxia in hypoxia-induced metastasis. *Clin Cancer Res* **13**, 1971–1978.

[30] Peters LJ, Brock WA, Chapman JD, and Wilson G (1998). Predictive assays of tumor radiocurability. *Am J Clin Oncol* **11**, 275–287.

[31] Rofstad EK and Måseide K (1998). Fraction of radiobiologically hypoxic cells in human melanoma xenografts measured by using single-cell survival, tumour growth delay and local tumour control as end points. *Br J Cancer* **78**, 893–898.

[32] Jain RK (1998). Determinants of tumor blood flow: a review. *Cancer Res* **48**, 2641–2658.

[33] Vaupel P, Kallinowski F, and Okunieff P (1989). Blood flow, oxygen and nutrient supply, and metabolic microenvironment of human tumors. *Cancer Res* **49**, 6449–6465.

[34] Bjørnæs I and Rofstad EK (2001). Microvascular permeability to macromolecules in human melanoma xenografts assessed by contrast-enhanced MRI—intertumor and intratumor heterogeneity. *Magn Reson Imaging* **19**, 723–730.

[35] Graff BA, Vangberg L, and Rofstad EK (2004). Quantitative assessment of uptake and distribution of iron oxide particles (NC 100150) in human melanoma xenografts by contrast-enhanced MRI. *Magn Reson Med* **51**, 727–735.

[36] Dewhirst MW, Cao Y, and Möller B (2008). Cycling hypoxia and free radicals regulate angiogenesis and radiotherapy response. *Nat Rev Cancer* **8**, 425–437.

[37] Brurberg KG, Gaustad JV, Mollatt CS, and Rofstad EK (2008). Temporal heterogeneity in blood supply in human tumor xenografts. *Neoplasia* **10**, 727–735.

[38] Boucher Y, Lee I, and Jain RK (1995). Lack of general correlation between interstitial fluid pressure and oxygen partial pressure in solid tumors. *Microvasc Res* **50**, 175–182.

[39] Tufto I, Lyng H, and Rofstad EK (1996). Interstitial fluid pressure, perfusion rate and oxygen tension in human melanoma xenografts. *Br J Cancer Suppl* **27**, S252–S255.

[40] Lunt SJ, Kalliomäki TMK, Brown A, Yang VX, Milosevic M, and Hill RP (2008). Interstitial fluid pressure, vascularity and metastasis in ectopc, orthotopic and spontaneous tumours. *BMC Cancer* **8**, 2.

[41] Heath VL and Bicknell R (2009). Anticancer strategies involving the vasculature. *Nat Rev Clin Oncol* **6**, 395–404.

[42] Jain RK (2005). Normalization of tumor vasculature: an emerging concept in antiangiogenic therapy. *Science* **307**, 58–62.